Int. J. Heat Mass Transfer. Vol. 25, No. 8, pp. 1103–1111, 1982
Printed in Great Britain

0017–9310/82/081103–09 $03.00/0
Pergamon Press Ltd.

THE METHOD OF CHARACTERISTICS APPLIED TO NUMERICAL SOLUTIONS OF GAS BUBBLE IMPLOSION AND FRAGMENTATION

W. M. SLUYTER, S. J. D. VAN STRALEN
Eindhoven University of Technology, Laboratory for Fluid Dynamics and Heat Transfer, Eindhoven, The Netherlands

and

W. ZIJL
B. V. Neratoom, P.O. Box 93244, 2509 AE Den Haag, The Netherlands

(*Received* 29 *June* 1981)

Abstract—The implosion of an ascending free gas bubble in an irrotational, incompressible and infinitely extended liquid has been studied numerically. The method of collocation combined with the method of characteristics to allow for multivalued solutions of the bubble radius has been applied. With this method fragmentation resulting from buoyancy-induced deviations from the spherical bubble shape has been described. In order to relate the results computed for gas bubbles to vapour bubbles, an estimation is presented for the minimum radial rate of vapour implosion where liquid inertia dominates temperature effects at the bubble boundary. In addition to a jet formation, the results show the detachment of small gas bubbles during the inertia-controlled mode of implosion.

NOMENCLATURE

a, liquid thermal diffusivity [$m^2 s^{-1}$]; expansion coefficient in series for velocity potential [$m^{3+2k} s^{-1}$];
a_1, vapour thermal diffusivity [$m s^{-1}$];
A_1, A_2, A_3, coefficient in characteristic equations (7) [m^{-1}], [$s m^{-1}$] and [—] respectively;
c_{p_1}, specific heat of vapour or gas at constant pressure [$J kg^{-1} K^{-1}$];
c_{v_1}, specific heat of vapour or gas at constant volume [$J kg^{-1} K^{-1}$];
F, N dimensional vector function, cf. equation (10);
g, gravitational acceleration [$m s^{-2}$];
K_1, K_2, K_3, characteristics;
K'_1, K'_2, base characteristics;
L, initial curve on integral surface I;
N, number of collocation points, $N = k + 1$;
p, liquid pressure [Pa];
p_1, vapour or gas pressure, [Pa];
Δp, pressure difference $= p_1 - p_\infty$ [Pa];
P_k, Legendre polynomial of order zero and degree k;
r, radial coordinate in spherical coordinate system [m];
R, bubble radius, coordinate of bubble wall [m];
R_0, undisturbed initial bubble radius [m];
s, parameter in equation (7);
t, time elapsed after start of bubble implosion [s];
Δt, time step at numerical integration [s];
T, absolute temperature of liquid [K];
T_1, absolute temperature of vapour [K];
$\boldsymbol{u}$, liquid velocity vector [$m s^{-1}$];
u, liquid velocity in radial direction [$m s^{-1}$];
u_1, gas velocity in radial direction [$m s^{-1}$];
V, volume of a gas or vapour bubble [m^3];
V_0, initial volume of a gas or vapour bubble [m^3].

Greek symbols

γ_1, Poisson's constant of the gas;
ε, disturbance in bubble radius [m];
ϑ, azimuthal angle in spherical coordinates;
λ, liquid coefficient of heat conduction [$W kg^{-1} m^{-1}$];
λ_1, coefficient of heat conduction in gaseous phase [$W kg^{-1} m^{-1}$];
ν, liquid kinematic viscosity [$m^2 s^{-1}$];
ρ, liquid density [$kg m^{-3}$];
ρ_1, saturated vapour or gas density [$kg m^{-3}$];
σ, surface tension coefficient [$kg s^{-2}$];
ϕ, liquid velocity potential [$m^2 s^{-1}$];
ω, circular frequency of bubble oscillations [s^{-1}].

Subscripts

i, j, integer number denoting collocation point, characterized by $R\{\vartheta_i(t)\} = R_i(t)$;
k, integer number in series expansion for velocity potential;
l, integer number denoting characteristic point characterized by $R\{\vartheta_l(t)\} = R_l(t)$;

max, maximum value;
min, minimum value;
tr, translation;
0, initial, at $t = 0$;
∞, far away from the bubble.

Superscripts

*, value, apply to $p_1 = p_\infty$;
˙, first differentiation with respect to time $[s^{-1}]$;
¨, second differentiation with respect to time $[s^{-2}]$.

INTRODUCTION

HEAT transfer during nucleate boiling is the subject of both experimental and theoretical investigations. For practical applications, one is interested in obtaining very high fluxes at low temperature differences between heating surface and bulk liquid. This can be realized under conditions of subcooled boiling, which occurs if the temperature of the bulk liquid is below the saturation temperature at ambient pressure. This situation often occurs in industrial processes.

Under subcooled boiling conditions, a vapour bubble which adheres to the superheated wall grows to a certain maximum size. This is due to a simultaneous implosion at the opposite side of the vapour–liquid interface (bubble wall) which is adjacent to subcooled bulk liquid. After departure the wall of the ascending bubble will deform during implosion.

In this paper, deformation means deviation from the spherical shape, and for free bubbles (i.e. bubbles in a liquid without solid walls) the deviations are caused by buoyancy forces only. For increasing degree of deformation, the bubble might even split up into smaller ones. This phenomenon is called fragmentation.

Although bubble growth and implosion have been extensively investigated, little is known about the physical process of bubble fragmentation. The transfer processes of mass, momentum and energy at the bubble wall are governed mainly by the flow field and temperature distribution in the liquid, whereas the flow- and temperature fields in the vapour phase are of second order importance. The flow- and temperature fields, in turn, are governed by the shape and motion of the bubble wall. The boundary conditions of the transfer processes for each region must be applied at the moving bubble wall. However, the position and the irregular shape of the bubble wall are not known beforehand but are part of the solution sought. Nevertheless, certain physical situations permit simplifications of the mathematics.

For example, the thermal effects at the bubble wall may be neglected if the motion of the bubble wall is controlled by inertia effects of the liquid. Similarly, the liquid can be treated as an incompressible fluid if the bubble wall velocity is much less than the sonic speed of the liquid. On the other hand, if thermal effects are dominant, the motion of the bubble wall is governed by a thin thermal liquid boundary layer.

In this paper, a method is developed to describe approximately the fragmentation phenomenon of one free gas bubble in an infinitely extended, incompressible and irrotational liquid. To solve this problem, we start from the basic equations of fluid dynamics and we confine ourself to the calculation of the liquid flow around the bubble. The resulting equations for the position and shape of the bubble boundary are solved numerically by means of the method of collocation combined with the method of characteristics. The latter method is applied to allow for multivalued solutions of the equation describing the (axially symmetric) bubble boundary as a function of azimuthal angle and time.

2. MATHEMATICAL FORMULATION

The basic equations of continuity and momentum, in combination with the relating boundary condition form the starting point of the mathematical treatment of the problem. The equation of state, $p_1 = p_1(\rho_1, T)$, for the gas or vapour in the bubble must be added to complete the set of equations. The boundary conditions apply to the situation of a free gas bubble in an infinitely extended liquid. In the case of a moving vapour–liquid interface, three boundary conditions must be presented in order to obtain a well-posed partial differential problem. These are obtained as follows: One condition for the normal stress discontinuity on the bubble boundary given by the Laplace equation [1] for the surface tension, one condition for the tangential stress discontinuity stating that tangential flow is introduced by surface tension gradients — the Marangoni effect—[2]—and one condition for conservation of mass at the liquid–vapour interface. In the latter case, it is assumed that the normal liquid flow velocity at the liquid–vapour interface equals the normal displacement rate of the bubble boundary. Under this condition, the expression for the conservation of mass at the liquid–vapour interface reduces to the well-known kinematic boundary condition that holds at an interface without phase transitions. As a result, only the equations for the liquid have been taken into account. Shockwaves occur in the liquid if, at the final stage of bubble implosion, the flow velocity at the bubble wall has the same order of magnitude as the liquid sonic speed. However this stage is not taken into consideration, so the liquid may be assumed to be incompressible i.e. both the liquid density, ρ, and kinematic viscosity, ν, are taken as constant. In this way the equations of continuity and energy have been uncoupled. The coupling between the momentum equation and the energy equation still exists via the pressure in the case of $p = p(T)$.

Under the restrictions mentioned above the theory for irrotational flow may be applied to the liquid

outside the thin boundary layer around the bubble and the continuity equation can be written as follows:

$$\nabla^2\phi = 0 \tag{1}$$

where $u = \nabla\phi$.

If only the phenomena are considered which occur during a sufficiently short time after the onset of motion of the bubble, that starts to translate (at $t = 0$), both the hydrodynamic boundary layer and the wake can be ignored. That is equation (1) holds and the condition for the tangential stress discontinuity can be disregarded. Under this restriction a well-posed problem was obtained. The momentum equation can then be integrated, resulting in the Bernoulli equation for the liquid pressure. Combination of the Laplace equation for the surface tension and the Bernoulli equation applied at the bubble boundary, $r = R(\vartheta, t)$ results in the so-called dynamic boundary condition. If the normal viscous stresses are neglected, the latter condition, written in spherical coordinates, and assuming rotational symmetry in the horizontal plane (see Fig. 1) is

$$\frac{\partial\phi}{\partial t} + \frac{1}{2}\left\{\left(\frac{\partial\phi}{\partial r}\right)^2 + \frac{1}{R^2}\left(\frac{\partial\phi}{\partial\vartheta}\right)^2\right\} + \frac{p_1 - p_\infty}{\rho} + gR\cos\vartheta - \frac{\sigma}{\rho}\left[\frac{\{1-(\partial^2R/\partial\vartheta^2)R^{-1}+2(\partial R/\partial\vartheta)^2R^{-2}\}}{R\{1+(\partial R/\partial\vartheta)^2R^{-2}\}^{3/2}} + \frac{1 - R^{-1}\cot\vartheta\,\partial R/\partial\vartheta}{R\{1+(\partial R/\partial\vartheta)^2R^{-2}\}}\right] = 0,\ r = R(\vartheta, t). \tag{2}$$

The kinematic boundary condition in the same coordinates is expressed by

$$\frac{\partial R}{\partial t} - \frac{\partial\phi}{\partial r} + \frac{1}{R^2}\frac{\partial\phi}{\partial\vartheta}\frac{\partial R}{\partial\vartheta} = 0,\ r = R(\vartheta, t). \tag{3}$$

Equation (1) and the boundary conditions (2) and (3) represent the set of equations to be solved in combination with prescribed initial conditions and gas pressure p_1.

It is important to emphasize here that equation (2), and in particular equation (3), may generally be applied to $r = R_m(\vartheta, t)$, which results in a multivalued solution for the bubble radius at a discrete angle and a fixed time (see Section 3.2. and Fig. 3).

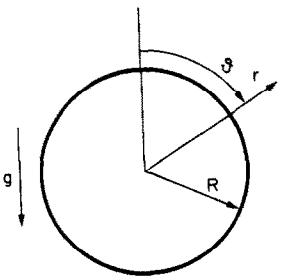

FIG. 1. Bubble with coordinates r, ϑ and R.

3. METHOD OF SOLUTION

3.1. *The collocation method*

The solution of equation (1) for rotational symmetry without singularities in $\vartheta = 0$ and $r \to \infty$ has the following form:

$$\phi(r, \vartheta, t) = \sum_{k=0}^{\infty} a_k(t)\frac{1}{r^{k+1}}P_k(\cos\vartheta). \tag{4}$$

For the velocity potential at discrete angles, ϑ_i, at the bubble boundary the following expression holds:

$$\frac{\mathrm{d}}{\mathrm{d}t}\phi(r, \vartheta_i, t) = \frac{\partial\phi}{\partial t} + \frac{\partial\phi}{\partial r}\frac{\mathrm{d}R}{\mathrm{d}t},\ r = R(\vartheta_i, t). \tag{5}$$

Substitution of equations (2) and (3) into equation (5) results in the dynamic boundary condition at $r = R(\vartheta_i, t)$ as it has been used for numerical integration.

An expression for the bubble radius in the form of a series expansion similar to equation (4) can only be used if the bubble radius is single-valued, i.e., if for every angle, ϑ, there is only one value $R(\vartheta)$. However, this latter restriction is not satisfied when bubble implosion and fragmentation are considered. In principle, the equations (2) and (4) in combination with an expression for the bubble radius, $R = R(\vartheta, t)$, and with the initial conditions and the condition for p_1, can be used to describe the flow-field and the coordinates of growing or imploding bubbles [4–7, 11]. Zijl *et al.* [4, 6, 11] and Joosten *et al.* [7] applied the (global, orthogonal) collocation method [10] to solve this set of equations numerically.

In equation (4) the series is truncated after N terms. The 1-dim. bubble boundary is discretized into N so-called collocation points, each of them representing a value of ϑ: the collocation angles ϑ_i.

The expansion coefficients, $a_k(t)$, $k = 0, \ldots N - 1$, are chosen in such a way, that only at these collocation angles, the solution of the truncated series (4) satisfies the boundary conditions equations (4) and (5). It is noted that the values of $\cos\vartheta_i$ are chosen as the zeros of a Legendre polynomial. In that case, convergence to the exact solution for $N \to \infty$ can be guaranteed [4, 8, 11].

3.2. *The method of characteristics*

Generally, the bubble radius $R = R(\vartheta, t)$ is not single-valued for an imploding bubble (see Fig. 3). Hence, the expansion of the bubble radius in a complete set of Legendre polynomials (see Section 3.1.) is useless for finding a multivalued solution of the bubble radius. Therefore, the kinematic boundary condition (3) will be considered as a quasi-linear partial differential equation (P.D.V.) of the following form:

$$A_1(\vartheta, t, R)\frac{\partial R}{\partial \vartheta} + A_2(\vartheta, t, R)\frac{\partial R}{\partial t} = A_3(\vartheta, t, R) \quad (6)$$

where A_1, A_2, A_3 are coefficients.

Suppose $R = R(\vartheta, t)$ is a solution of the P.D.V. (6). This solution corresponds to an integral surface in the 3-dim. (ϑ, t, R)-continuum with orthogonal coordinates. On the integral surface, characteristic curves can be constructed [9]. By means of the parametric representation, $\vartheta = \vartheta(s)$, $t = t(s)$, $R = R(s)$, of these characteristics, the equations for the characteristics take the following form:

$$\frac{d\vartheta}{ds} = A_1(\vartheta, t, R), \frac{dt}{ds} = A_2(\vartheta, t), \frac{dR}{ds} = A_3(\vartheta, t, R). \quad (7)$$

The uniqueness of equation (7) is guaranteed if initial conditions are prescribed on an initial curve which is not a characteristic itself i.e.

$$\vartheta(s_0) = \vartheta_0, t(s_0) = t_0, R(s_0) = R_0.$$

Now equations (6) and (7) will be compared with equation (3). Substitution of $s = t$ into equation (7) results in the characteristics of equation (3) and they have the following form:

$$\frac{d\vartheta}{dt} = \frac{1}{R^2}\frac{\partial \phi}{\partial \vartheta}. \quad (8)$$

$$\frac{dR}{dt} = \left(\frac{\partial \phi}{\partial r}\right)_{r=R}. \quad (9)$$

Using equations (8) and (9), a multivalued solution of the bubble radius is possible and finds expression in the intersection of the base characteristics i.e. in the projections of the characteristics in the ϑ, t-plane (Fig. 2). Consequently, when using the method described above, the deformed bubble boundary may have different bubble radii at one discrete angle and one fixed time (Fig. 3).

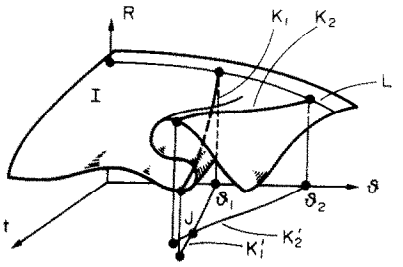

FIG. 2. Integral surface I with characteristics K_1 and K_2 from the initial curve L at ϑ_1 respectively ϑ_2. The base characteristics K'_1 and K'_2 show a multivated solution of $R(\vartheta, t)$ in the point of intersection J.

4. THE NUMERICAL METHOD

The collocation method described in Section 3.1. is applied to solve the equations (2)–(4) and results in a set of N coupled, non-linear ordinary differential equations for the velocity potential

$$\frac{d}{dt}\phi_i = F(R_j, \phi_j)_{j=0}^{N-1}, i = 0(1)N - 1 \quad (10)$$

where

$$\phi_i(t) = \phi\{R_i(t), \vartheta_i(t)\} = \sum_{k=0}^{N} \left[\left\{\frac{1}{R_i(t)}\right\}^{k+1} P_k(\cos \vartheta_i)\right] a_k(t) \quad (11)$$

with

$$R_i(t) = R(\vartheta_i, t).$$

The matrix equation (11) must be solved for every timestep. This can be performed by numerical standard routine (LU decomposition). The initial conditions are

$$\phi_i(0) = 0, R_i(0) = 0. \quad (12)$$

However, at the collocation points, where the velocity potential (11) has to be determined for reasons mentioned in Section 3.1, an equation for the bubble radius, $R_i(t)$, is missing. Hence a linear interpolation procedure is introduced.

$$R_i = \frac{R_{l+1}\Delta\vartheta_l + R_l\Delta\vartheta_{l+1}}{\Delta\vartheta_l + \Delta\vartheta_{l+1}}, \quad \left\{\begin{matrix}\vartheta_l < \vartheta_i < \vartheta_{l+1} \\ l = 1(1)N + 1\end{matrix}\right\} \quad (13)$$

where $R_i(t) = R(\vartheta_i, t)$ denotes the characteristic bubble radius, i.e. the coordinate of a characteristic point that coincides with both the bubble wall and the characteristic.

The discrete interpolation angles, $\Delta\vartheta_l$ and $\Delta\vartheta_{l+1}$, chosen between the collocation angles, serve as weighting factors such that $R_i(t)$ coincides the adjacent characteristic radius for $\Delta\vartheta_l = 0$ or $\Delta\vartheta_{l+1} = 0$. Moreover, even for large deformations of the bubble wall, the volume of the bubble can be exactly de-

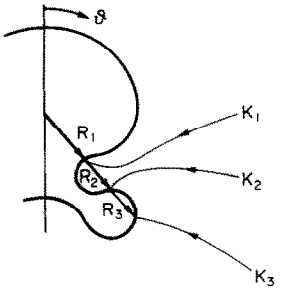

FIG. 3. Three-valued solution of the bubble radius: R_1, R_2 and R_3. The characteristics K_1, K_2 and K_3 do not intersect.

termined by rotationally symmetric integration if the 1-dim. bubble wall is described by R_i of equation (13) with continuous variable $\Delta\vartheta_i$ [12].

The numerical procedure to be used is as follows:

(i) Initially the coefficients $a_k(0)$ will be determined by means of equations (11) and (12), and the derivatives $\partial\phi_i/\partial\vartheta$ and $\partial\phi_i/\partial r$ can be calculated analytically.

(ii) Initially the characteristic points are chosen at the bubble wall between the collocation points. The derivative $\partial\phi_i/\partial\vartheta$ and $\partial\phi_i/\partial r$ will be calculated using the matrices P_k (cos ϑ_i), $\{dp(\cos\vartheta)/d\vartheta\}_i$.

(iii) After each timestep, Δt, the new characteristic radii will be determined with equations (8) and (9). In the examples presented in this paper a simple Euler integration method has been used.

(iv) Both the bubble radii and their derivatives have been determined at the collocation angles applying linear interpolation see equation (13).

(v) $d\phi_i/dt$ has been calculated using equation (5) for time t. Subsequently, using the Euler method, the new ϕ_i has been calculated at a time $t + \Delta t$ at the collocation points. After this, the procedure was repeated for each timestep consecutively.

5. COMPRESSIBILITY EFFECTS

5.1. *Spherically symmetric vapour bubble implosion*

It is significant to compare the numerical results to those of suitable experiments on vapour bubbles. At present, only the buoyancy-induced deformation of a translating bubble has been taken into account (see Section 2). Consequently, thermal and diffusive effects are neglected in the analysis. However, for an imploding vapour bubble, heat diffusion will be of importance. In this case, heat of condensation is liberated at the bubble boundary and the energy has to be involved in the analysis. Nevertheless, the vapour in the bubble can be treated as a compressible gas if no condensation occurs. Therefore, to conclude whether the numerical results are applicable to vapour bubbles, it is necessary to check during which stage of the bubble implosion the thermal and compressibility effects are important.

In this respect, the behaviour of the gas or vapour phase for a radially imploding (or expanding) bubble in a subcooled (or superheated) liquid will be considered.

5.2. *Compressible bubbles*

Since $\rho_1 \ll \rho$, disturbances in the pressure of the gaseous phase within a closed volume are damped away much more rapidly than in the liquid.

Consequently, if viscosity effects are neglected, the pressure in the gaseous phase may be assumed to be homogeneous i.e.

$$\nabla p_1 = 0. \tag{14}$$

For simplicity a spherical bubble is considered. Conservation of total mass at the spherical liquid–vapour interface results in

$$\rho_1(u_1 - \dot{R}) = \rho(u - \dot{R}). \tag{15}$$

In the case under consideration where phase transition, i.e. condensation, at the interface is excluded, equation (15), under the condition $\rho_1 \ll \rho$, becomes equivalent to the well-known kinematic boundary condition $u = \dot{R}$.

The thermal boundary condition at the vapour–liquid interface $r = R(t)$ is given by

$$\lambda\left(\frac{\partial T}{\partial r}\right)_{r=R} - \lambda_1\left(\frac{\partial T_1}{\partial r}\right)_{r=R} = \rho_1 l(\dot{R} - u_1). \tag{16}$$

Equation (16) expresses that the heat required for condensation or evaporation must be removed or supplied by conduction through the liquid and the vapour adjacent to the bubble boundary. With the help of the equations of continuity and energy for the vapour taken as an ideal gas without viscous dissipation, in combination with equation (14), Cho and Seban [13] derived the following expression for the radial vapour velocity at the interface:

$$u_1 = \frac{1}{p_1}\left\{\frac{c_{p_1} - c_{v_1}}{c_{p_1}}\left(\lambda_1\frac{\partial T_1}{\partial r}\right)_{r=R} - \frac{dp_1}{dt}\frac{R}{3}\frac{c_{v_1}}{c_{p_1}}\right\}, \quad r = R. \tag{17}$$

Under the assumption $\lambda_1 \ll \lambda$ and $a_1 \gg a$, the temperature differences in the vapour can be neglected. Combination of equation (16) and equation (17) results then in

$$\lambda\left(\frac{\partial T}{\partial r}\right)_{r=R} = \rho_1 l\left(\dot{R} + \frac{dp_1}{dt}\frac{R}{3p_1}\frac{c_{v_1}}{c_{p_1}}\right), \quad r = R. \tag{18}$$

When the absolute value of the first term between brackets in the RHS of equation (18) is much larger than the second one, condensation or evaporation occurs at the bubble boundary during implosion or growth respectively and compressibility effects may be neglected. However, if $\lambda(\partial T/\partial r)_{r=R} = 0$ in the LHS of equation (18), heat transfer effects at the bubble boundary may be neglected and compressibility of the vapour dominates implosion or growth. According to equation (18), for sufficiently small disturbances in the vapour pressure, the vapour can thus be treated as a compressible gas, if

$$\frac{1}{R}\frac{dR}{dt} \simeq -\frac{1}{3p_\infty\gamma_1}\frac{dp_1}{dt}. \tag{19}$$

In turn, if equation (19) is satisfied, the implosion is governed by liquid inertia and the bubble radius is

given by the so-called Rayleigh–Plesset equation [14]

$$\ddot{R}R + \frac{3}{2}\dot{R}^2 = \frac{p_1 - p_\infty}{\rho} - \frac{2\sigma}{\rho R}. \tag{20}$$

This equation can also be derived from equation (5) and equation (4) for $k = 0$, i.e. in case of a spherically symmetric flow field.

Let the perturbation in the bubble radius be represented by

$$R(t) = R_0 + \varepsilon(t). \tag{21}$$

In the following discussion it will be assumed that $|\varepsilon(t)| \ll R_0$ in such a way, that terms in powers of ε, $\dot{\varepsilon}$, and higher derivatives greater than one may be neglected. Substitution of equation (21) into equation (20) and linearization results in

$$R_0\ddot{\varepsilon} = \frac{p_1 - p_\infty}{\rho} \tag{22}$$

if the surface tension term has been neglected.

Comparison of equation (22) with the first and second terms between brackets in the RHS of equation (18) shows that these terms have amplitudes of $\ddot{\varepsilon}(t_0)/\omega$ and $\ddot{\varepsilon}(t_0)\omega\rho R_0^2/3p_\infty\gamma_1$ respectively. Consequently, the vapour can be treated as a compressible gas if $\{\rho R_0^2\omega\ddot{\varepsilon}(t_0)/\gamma_1^3 p_\infty\} \gg \{\ddot{\varepsilon}(t_0)/\omega\}$ or

$$\omega \simeq \left(\frac{3\gamma_1 p_\infty}{\rho}\right)^{1/2}\frac{1}{R_0}. \tag{23}$$

Provided that $(1/R_0)|\dot{R}| \simeq \omega$, substitution of ω into equation (23) results in $|dR/dt| \simeq (3p_\infty\gamma_1/\rho)^{1/2}$, consequently, it follows that the vapour behaves as a compressible gas if

$$\left|\frac{dR}{dt}\right| \geq \left(\frac{3\gamma_1 p_\infty}{\rho}\right)^{1/2}. \tag{24}$$

On the other hand, if $|dR/dt| \ll (3p_\infty\gamma_1/\rho)^{1/2}$, mainly condensation occurs and compressibility effects of the vapour may be neglected. Supposing that a point fixed at the imploding bubble wall follows the largest deformation from onset. Possibly, such a deformation, or the resulting fragmentation, can be expected at vapour bubbles if the radial velocity of the bubble wall at that point satisfies condition (24). Nevertheless all examples presented in Section 6 satisfy condition (24).

6. NUMERICAL EXAMPLES

6.1. *Rotationally symmetric bubble implosion*

For gas bubbles, the pressure p_1 in equation (2) is replaced by the isentropic law

$$p_1(t) = p_{1,0}\{V_0/V(t)\}^{\gamma_1}. \tag{25}$$

We consider the hypothetical case of $\gamma_1 = 1$, i.e. when equation (25) represents the ideal gas law, this case applies to isothermal (gas) implosion. During implosion, the internal pressure is increasing according to equation (25) and, due to the inertia of the liquid, it exceeds the liquid pressure p_∞ after a certain time. Consequently, the bubble will start growing and, for sufficiently large times, the bubble volume oscillates. Here, only the first implosion stage has been considered with $p_1(t)$ given by equation (25). However, the bubble will hardly implode for realistic values of the internal pressure, $p_1(t)$, and the liquid pressure, p_∞, (e.g. for $p_\infty = 100$ kPa and $p_1(0) = 99$ kPa, the ratio $R^*/R_0 \approx 0.99$, where $R^* = R(t^*)$ is the radius of the spherical bubble at advanced implosion with internal pressure $p_1(t^*) = p_\infty$). Therefore, some calculations have been made at a pressure difference $\Delta p = p_1 - p_\infty = p_{1,0} - p_\infty =$ constant, i.e. the implosion rate has not been slowed down by the compressibility of the gas (Figs. 6 and 7). Figs. 4–6 show nearly the same bubble shape for both isothermal implosion and implosion with constant Δp. Therefore, it seems to be justified to study bubble deformation during implosion at constant internal pressure. Since, due to buoyancy (see Section 2), the bubble translates and the origin of the coordinate system has been fixed at the bubble centre. The translation velocity of the origin u_{tr} (initially $u_{tr} = 0$) is positive in the direction opposite to gravitational acceleration and it is defined by $\frac{1}{2}\{\dot{R}(\pi, t) - \dot{R}(0, t)\}$. In the figures the origins coincide for the different implosion stages. Because of the rotational symmetry (see Section 2) the bubble shape at various instants has

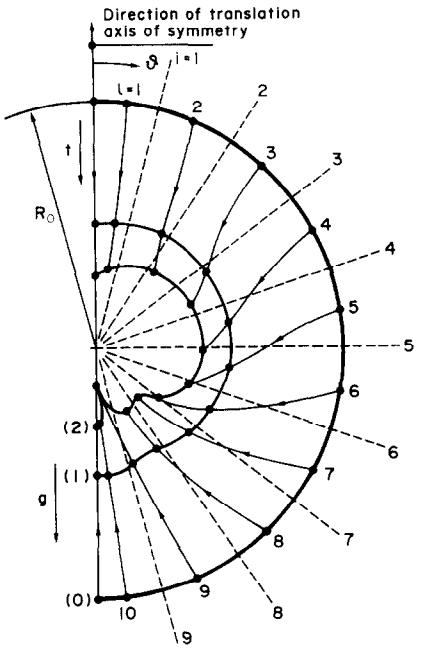

FIG. 4. Numerically calculated profile of a free translating isothermal gas bubble, imploding in a pressure field at various instants, $N = 9$. Curve (1): $p_1 = 1.9$ kPa, $t_1 = 10.0000$ ms, Curve (2): $p_1 = 4.55$ kPa, $t_2 = 10.983$ ms, $p_\infty = 1$ kPa, $p_{1,0} = 0.25$ kPa, $R_0 = 10$ mm, $\gamma_1 = 1$, $\rho = 10^3$ kg m^{-3} $g = 9.81$ m s^{-2}.

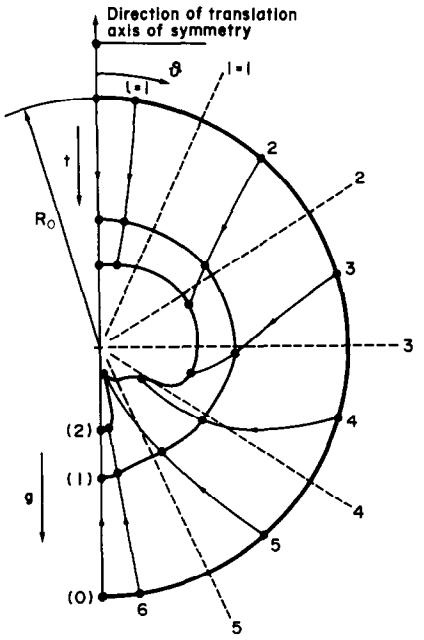

FIG. 5. Numerically calculated profile of a free translating isothermal gas bubble, imploding in a pressure field at various instants, $N = 5$. Curve (1): $p_1 = 1.77\,\text{kPa}$, $t_1 = 9.950\,\text{ms}$, Curve (2): $p_1 = 5.88\,\text{kPa}$, $t_1 = 11.021\,\text{ms}$, other values as Fig. 4.

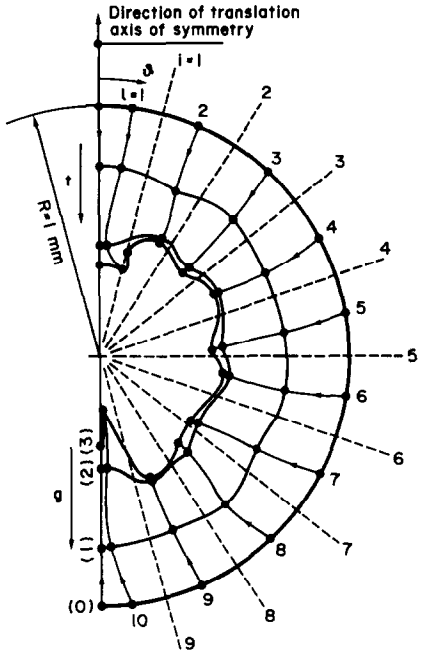

FIG. 7. Numerically calculated profile of a free translating hollow cavity, impliding in a pressure field at various instants, $N = 9$. Onset of detachment as well at the top of the bubble as at its rear. Curve (1) $t_1 = 1.0970\,\text{ms}$, Curve (2) $t_2 = 1.0977\,\text{ms}$, Curve (3) $t_3 = 1.0977\,\text{ms}$. $p_\infty = 100\,\text{kPa}$, $p_1 = 20\,\text{kPa}$, other values as Fig. 4.

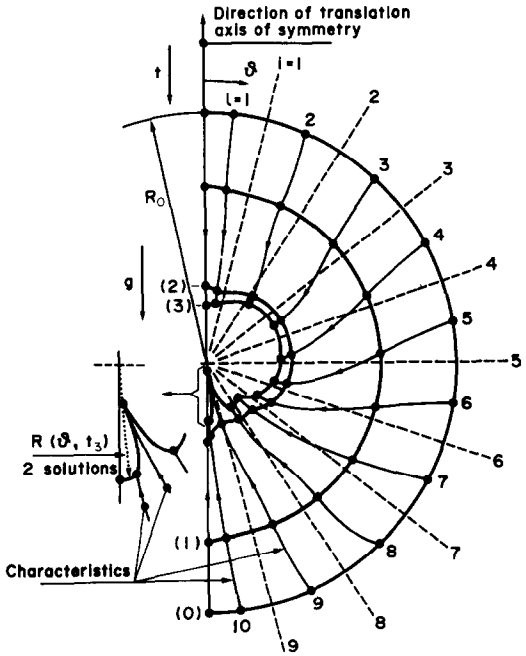

FIG. 6. Numerically calculated profile of a free translating hollow cavity, imploding in a pressure field at various instants, $N = 9$. A small bubble detaching at its rear. Curve (1) $t_1 = 7.000\,\text{ms}$, Curve (2) $t_2 = 9.000\,\text{ms}$ Curve (3) $t_3 = 9.092\,\text{ms}$. $p_1 = 0\,\text{kPa}$, other values as Fig. 4.

been drawn for values of ϑ in the interval $[0, \pi]$. Initially [situation (0)], $N + 1$ characteristic points R_l are chosen at the bubble wall. The radially directed drawn curves are characteristics, the dashed curves are the collocation angles, see Figs. 4–8.

The examples that follow have been calculated with the Burroughs B-6700 computer of the Eindhoven University of Technology.

6.2. *Compressible bubbles*

Figure 4 shows an imploding gas bubble at an initial pressure $p_1(t)$ according to equation (25). The maximum radial velocity of the bubble wall $|\dot{R}_l(t)|_{\max}$ for $l = 9$ and $t_2 \leq t \leq t_1$ shows physically realistic values around the sonic speed of water ($1.5.10^3\,\text{m s}^{-1}$) while $|\dot{R}_l(t_1)|_{\min} = 2.13\,\text{m s}^{-1}$ for $l = 2$ and $|\dot{R}_l(t_2)|_{\min} = 1.90\,\text{m s}^{-1}$ for $l = 3$. Also fragmentation occurs: a small bubble detaches at the rear of the original one (see also the inset of Fig. 6). For $t = t_2$, the implosion rate has almost been slowed down completely. The imploding gas bubble, shown in Fig. 5, differs only with the conditions used in Fig. 4 for $N = 5$ although both figures show nearly the same bubble shape. Also the numerically calculated radial velocities of the bubble wall agree for the various instants of Figs. 4 and 5. They amount for $t = t_1$, $|\dot{R}_{l=9}(t_1)|_{\max} = 2.1\,\text{m s}^{-1}$ (Fig. 4) respectively $|\dot{R}_{l=5}(t_1)|_{\max} = 2.3\,\text{m s}^{-1}$ (Fig. 5). The corresponding theoretical value, given by equation (24) for both Fig. 4 and Fig. 5 [see text, Section 5.2. after equation (24)] is $\dot{R} = 1.7\,\text{m s}^{-1}$. Both Fig. 4 and Fig. 5 show a multivated solution for $t = t_2$ because $\vartheta_{l=9} < \vartheta_{l=10}$ and $\vartheta_{l=5} < \vartheta_{l=6}$ respectively.

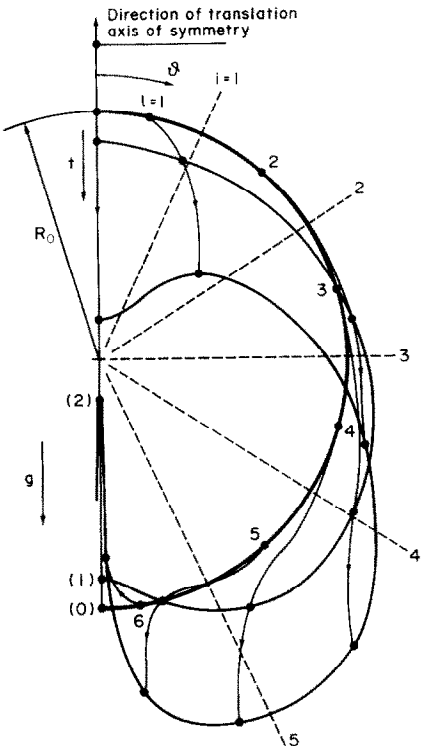

FIG. 8. Deformation of an accelerated bubble at a pressure of 1 kPa; tongue formation occurs at the rear of the bubble, $N = 5$. Curve (1) $t_1 = 23.500$ ms, Curve (2) $t_2 = 24.813$ ms, $p_1 = p_\infty = 1$ kPa other values as Fig. 4.

6.3. *Imploding bubbles with constant internal pressure*

Figure 6 shows an imploding hollow cavity. This shows that the implosion rate has not been slowed down by the compressibility of the gas. However, there is a very good agreement with the bubble shapes shown in Fig. 4 and Fig. 5 (see Section 6.1.). The inset of Fig. 6 for $t = t_3$ shows clearly a multivalued solution of the bubble radius (dotted line) the detachment of a small bubble at the rear i.e. fragmentation. The maximum radial velocity of the bubble wall $|\dot{R}_l(t)|_{\max} = 4.47 \times 10^{10}\,\mathrm{m\,s^{-1}}$ for $l = 9, t = t_3$ and $7.0\,\mathrm{m\,s^{-1}}$ for $l = 9, t = t_2$. For all instants $|\dot{R}_l(t)|_{\min} < 3.66\,\mathrm{m\,s^{-1}}$.

Figure 7 shows an imploding gas bubble with constant internal pressure. Here, in contradistinction to Fig. 6, deformation of the bubble wall occurs for $R < 10^{-3}$ m due to the large value of $|\Delta p| = 80$ kPa. There multivalued solution of $R(\vartheta, t_3)$ because $\vartheta_{i=1} < \vartheta_{i=1}$. The maximum radial velocity of the bubble wall $|\dot{R}_l(t)|_{\max} = 3.03 \times 10^6\,\mathrm{m\,s^{-1}}$ for $l = 10, t = t_3$ and $1.76 \times 10^3\,\mathrm{m\,s^{-1}}$ for $l = 10, t = t_2$. For all instants $|\dot{R}_l(t)|_{\min} < 470.1\,\mathrm{m\,s^{-1}}$ holds.

Figure 8 shows the deformation of the bubble wall of an accelerated ascending bubble for $\Delta p = 0$. The deformation can be followed via the characteristics. The ultimate shape for $t > 24.813$ ms is a toroidal bubble, in agreement with experimental results of Walters and Davidson [16].

Finally, the calculated initial acceleration for Figs. 4–8 equals $2g$ in agreement with Walters and Davidson [16] and Zijl [5].

7. CONCLUSIONS

For almost all calculated examples, the maximum radial velocity of the bubble wall at large rates of deformation or fragmentation is of the order of magnitude of the liquid sonic speed. When this occurs the compressibility of the liquid, which has been neglected in this paper, needs to be taken into account. Otherwise it is observed that large rates of deformation or fragmentation of the bubble wall occur in the situation where bubble implosion is controlled by inertia of the liquid. Plesset and Mitchell [17] investigated the stability of perturbation terms of expanding and collapsing bubbles, assuming the pressure inside the bubble to be constant. They conclude that an expanding bubble is stable while an imploding one is not. In the latter case the distortion amplitude grows as $R^{-1.4}$ when the bubble radius R tends to zero. The buoyancy term $gR\cos\vartheta$ in equation (2) accounts for deformation only and not for instability.

Evidently, the initial perturbations, expressed by the coefficients $a_k(0) \neq 0, k = 1(1)N, g \equiv 0$, agree with the so-called Taylor instabilities [18]. A combination of gravitational effect and Taylor instability results in the presented deformations. For advanced implosion, e.g. for decreasing R, the latter effect dominates the effect of gravitation ($gR\cos\vartheta$) in agreement with the numerical examples. Fragmentation of vapour or gas bubbles can be described with the method of characteristics combined with the method of collocation as presented here. Detachment of small bubbles from the original bubble occurs in combination with well-known jet formation at the rear of the bubble: the accompanying translation velocity u_{tr} changes very fast.

REFERENCES

1. L. D. Landau and E. M. Lifshitz, *Fluid Mechanics*. Pergamon Press, Oxford (1959).
2. V. G. Levich, *Physiochemical Hydrodynamics*. Prentice-Hall, Engelwood Cliffs, New Jersey (1962).
3. G. K. Batchelor, *An Introduction to Fluid Dynamics*. Cambridge University Press, Cambridge (1976).
4. W. Zijl, The hydrodynamics of vapour and gas bubbles by numerical approximations methods, in *Boiling Phenomena*, (edited by S. J. D. van Stralen and R. Cole). Hemisphere, Washington D. C. (1979). A more detailed review is given in [11].
5. W. Zijl, Global collocation approximations of the flow and temperature fields around a gas and vapour bubble, *Int. J. Heat Mass Transfer* **20**, 487–498 (1977).
6. W. Zijl, F. J. M. Ramakers and S. J. D. van Stralen, Global numerical solutions of growth and departure of a vapour bubble at a horizontal superheated wall in a pure liquid and a binary mixture, *Int. J. Heat Mass Transfer* **22**, 401–420 (1979).
7. J. G. H. Joosten, W. Zijl and S. J. D. van Stralen, Growth of a vapour bubble in combined gravitational and non-uniform temperature fields, *Int. J. Heat Mass Transfer* **21**, 15–23 (1978).
8. L. Fox and I. B. Parker, *Chebychev Polynomials in*

Numerical Analysis. Oxford University Press, London (1968).
9. R. Courant and D. Hilbert, *Methods of Mathematical Physics*, Vol. 2, *Partial Differential Equations*. Interscience, New York (1962).
10. B. A. Finlayson, The method of weighted residuals and variational principles, in *Mathematics in Science and Engineering*, Vol. 87. Academic Press, New York (1972).
11. W. Zijl, Departure of a bubble growing on a horizontal wall, Ph.D. thesis, University of Technology, Eindhoven, The Netherlands.
12. W. M. Sluyter, Master thesis, Eindhoven University of Technology (1978).
13. S. M. Cho and R. A. Seban, On some aspects of steam bubble collapse, *Am. Soc. Mech. Engrs* Series C, *J. Heat Transfer* **91**, 537–542 (1969).
14. Lord Rayleigh, On the pressure developed in a liquid during the collapse of a spherical cavity, *Phil. Mag.* **34**, 94–98 (1917).
15. S. M. Cho and R. A. Seban, Oscillation of a gas bubble in an infinite fluid, *Am. Soc. Mech. Engrs*, Series C, *J. Heat Transfer* **91**, 157–159 (1969).
16. J. T. K. Walters and J. F. Davidson, The initial motion of a gas bubble formed in an inviscid liquid, *J. Fluid Mech.* **17**, 321–337 (1963).
17. M. S. Plesset and T. P. Mitchell, On the stability of the spherical shape of a vapour cavity in a liquid, *Q. Appl. Math.* **13**, 419–430 (1956).
18. G. I. Taylor, The instability of liquid surfaces when accelerated in a direction perpendicular to their planes, *Proc. R. Soc., Lond.* **A201**, 192–196 (1950).

APPLICATION DE LA METHODE DES CARACTERISTIQUES A LA RESOLUTION NUMERIQUE DE L'IMPLOSION ET DE LA FRAGMENTATION DES BULLES DE GAZ

Résumé—On étudie numériquement l'implosion d'une bulle ascendante de gaz dans un liquide irrotationnel, incompressible et infiniment étendu. La méthode de collocation combinée avec la méthode des caractéristiques a été appliquée aux solutions du rayon de la bulle. Avec cette méthode est décrite la fragmentation résultant des déviations, induites par les forces d'Archimède, à partir de la forme sphérique de la bulle. De façon à relier les résultats calculés pour les bulles de gaz et de vapeur, on présente une estimation de la vitesse radiale minimale d'implosion quand l'inertie de liquide domine les effets de température à la frontière de la bulle. Les résultats montrent qu'en plus de la formation d'un jet, il y a un détachement de petites bulles de gaz pendant le mode d'implosion contrôlé par l'inertie.

ANWENDUNG DES CHARAKTERISTIKEN-VERFAHRENS BEI DER NUMERISCHEN LÖSUNG DES IMPLOSIONS- UND FRAGMENTATIONS-VERLAUFS VON GASBLASEN

Zusammenfassung—Die Implosion einer aufsteigenden freien Gasblase in einer rotationsfreien, inkompressiblen, unendlich ausgedehnten Flüssigkeit wurde numerisch untersucht. Um mehrdeutige Lösungen für den Blassenradius in Betracht zu ziehen, wurde die mit dem Charakteristiken-Verfahren kombinierte Kollokations-Methode angewandt. Mit diesem Verfahren wurde die durch auftriebsbedingte Abweichung von der Kugelform hervorgerufene Fragmentation beschrieben. Um die Beziehung der für Gasblassen berechneten Ergebnisse zu Dampfblasen herzustellen, wird für die minimale radiale Dampf-Implosions-Geschwindigkeit, bei der die Trägheits-Effekte der Flüssigkeit gegenüber thermischen Effekten an der Blasengrenze noch überwiegen, eine Abschätzung angegeben. Neben der Ausbildung eines Strahls zeigen die Rechenergebnisse die Ablösung kleiner Gasblasen während der durch Trägheitskräfte bestimmten Implosionsphase.

ЧИСЛЕННОЕ ИССЛЕДОВАНИЕ ПРОЦЕССА СХЛОПЫВАНИЯ И ДРОБЛЕНИЯ ГАЗОВЫХ ПУЗЫРЬКОВ МЕТОДОМ ХАРАКТЕРИСТИК

Аннотация — Проведено численное исследование схлопывания свободно всплывающего газового пузырька в неограниченном объеме неподвижной несжимаемой жидкости. В решении задачи о радиусе пузырьков использовался метод коллокаций в комбинации с методом характеристик, что позволило получить несколько решений. Это дало возможность описать дробление пузырьков, происходящее в результате их отклонения от сферической формы под действием подъемных сил. Для обобщения результатов, полученных для газовых пузырьков, на случай паровых пузырьков проведена оценка минимальной радиальной скорости испарения внутрь пузырька, когда инерция жидкости превалирует над температурными эффектами на границе. Результаты показывают, что помимо образования струи в течение всего периода схлопывания происходит отрыв небольших газовых пузырьков.